

"The submitted manuscript has been authorized by a contractor of the U.S. Government under contract No. DE-AC05-84OR21400. Accordingly, the U.S. Government retains a nonexclusive, royalty-free license to publish or reproduce the published form of this contribution, or allow others to do so, for U.S. Government purposes."

ION BEAM INDUCED DIFFUSION AND CRYSTALLIZATION  
IN HIGH DOSE Er IMPLANTED Si CONF-900936--19  
DE91 002869

A.GOLANSKI\*, W.H.CHRISTIE, M.D.GALLOWAY, J.L.PARK,  
S.J.PENNYCOOK, D.B.POKER, J.L.MOORE, H.E.HARMON and  
C.W.WHITE

Oak Ridge National Laboratory, Oak Ridge, Tn.37831, USA.

\* Centre National d'Etudes des Telecommunications, B.P.98.  
38240 Meylan, France.

ABSTRACT

High doses ( $1 \times 10^{16}$  -  $1 \times 10^{17}$   $\text{cm}^{-2}$ ) of 145 keV and 175 keV Er<sup>+</sup> ions were implanted into single-crystal Si using implantation temperatures ( $T_i$ ) between room temperature and 500°C. Implanted samples were subsequently annealed using thermal annealing at 800°C under vacuum as well as a 1 MeV As<sup>+</sup> ion beam assisted annealing (IBAA) at 300°C. During Er<sup>+</sup> implantation, we find evidence for ion beam induced mobility for  $T_i$  as low as 300°C. A measurable redistribution of the implanted Er also occurs during the IBAA for Er doses greater than  $5 \times 10^{16}$   $\text{cm}^{-2}$ . During Er<sup>+</sup> implantation at  $T_i > 300^\circ\text{C}$  a polycrystalline  $\text{ErSi}_2$  phase is formed. For  $T_i > 400^\circ\text{C}$  the coherent precipitation of  $\text{ErSi}_2$  phase occurs within the crystalline Si matrix. During subsequent thermal annealing of samples implanted at  $T_i > 400^\circ\text{C}$ , the Er distribution narrows due to Ostwald ripening, and preferential allignment occurs to form a discontinuous buried layer of a single crystalline Er silicide.

Research sponsored by the Division of Materials Sciences, U.S. Department of Energy under contract DE-AC05-84OR21400 with Martin Marietta Energy Systems, Inc.

DISTRIBUTION OF THIS DOCUMENT IS UNLIMITED

MASTER

## INTRODUCTION

Metal silicides have been widely used in VLSI technology to form uniform and thermally stable contacts, interconnects and low-resistivity gates for high speed applications [1,2 and ref.therein]. Recently the rare-earth silicides have attracted considerable attention because they form the lowest known Schottky barrier heights on n-type Si [3,4] and appear to be potentially attractive as low contact resistance materials for high integration density device structures. Silicides of Tb, Ho, Er, Tm, Yb, Lu and Y have been shown to grow by solid phase epitaxy [5,6], while silicides of Tm, Yb, Lu, Gd and Dy can be formed epitaxially in liquid phase reaction using electron beam melting [5]. Ultra-high vacuum co-deposition of Er and Si, followed by an appropriate thermal annealing has also been successfully used to form single crystal Er silicide layers [1,2]. Although a variety of buried silicides has been formed using ion beam synthesis [7 and ref.therein], only a few results concerning implantation of rare earth elements have been reported so far [8]. One of the potential difficulties related to the ion beam synthesis of these compounds is a relatively high theoretical value of the sputtering yield  $Y$  ( $Y=5.6$  for 145 keV  $Er^+$ ) which may act as a dose-limiting factor. However, a substantial decrease of  $Y$  values has been observed for implantations performed at elevated temperatures [9]. The physical mechanism responsible is believed to be a combination of thermally activated (or radiation-enhanced) diffusion and compound formation leading to an increase in

the effective surface binding energy. During formation of erbium di-silicide by interaction of deposited metallic thin films with single crystal Si, the silicon atoms are the dominant diffusing species and the metal atoms do not acquire any significant mobility up to temperatures of 700-800°C [10], a temperature which is considerably in excess of the silicide formation temperatures [6]. One might therefore expect the implanted Er distributions to be stable for the  $T_i$  range used in this work. We have systematically investigated implanted Er distributions for a variety of the  $T_i$  values to determine whether beam induced or chemical effects are significant in the case of Er implantation into single crystal Si.

#### EXPERIMENTAL

Er ions for implantation were produced in a sputter ion source. Various doses were implanted at 145 keV or 170 keV into single crystal (111) and (100) oriented Si samples. Careful precautions were taken in order to minimize channeling effects during implantation. The substrate temperature  $T_i$  was regulated within the range  $RT < T_i < 520^\circ C$  using a heater located within the sample holder. For most of the implants ion beam current density was below  $10 \mu A/cm^2$  in order to minimize beam heating effects. Implanted samples were subsequently annealed at  $800^\circ C$  for 1 hour in a vacuum of  $8 \times 10^{-7}$  Torr. Ion beam assisted annealing (IBAA) was carried out using 1.02 MeV As ions. The beam current density was close to  $8 \mu A/cm^2$ . The substrate temperature

was monitored during the implantation and maintained close to 300°C. RBS-ion channeling analysis (using 1.2 MeV He ions) and cross-sectional transmission electron microscopy (XTEM) were used to characterize the implanted and annealed samples. X-ray diffraction patterns were measured using a Huber 651/652 Guinier thin film diffractometer. Selected samples were analysed using secondary ion mass spectrometry (SIMS).

#### RESULTS AND DISCUSSION.

##### 1. Ion beam induced diffusion and segregation.

For 145 KeV Er<sup>+</sup> ions the theoretical value of the retention R (defined as the fraction of the implanted dose retained in spite of the sputtering erosion) calculated using the Profile code [11] varies from 100% at a dose of  $1 \times 10^{16} \text{ cm}^{-2}$  to 51% at a dose of  $1 \times 10^{17} \text{ cm}^{-2}$ . The dose of  $1 \times 10^{16} \text{ cm}^{-2}$  was therefore used for a systematic investigation of the  $R_p$  values for a variety of implantation temperatures  $T_i$ . The results are summarised in the Fig.1 where the average experimental  $R_p(\text{ex})$  values, normalised to the theoretical value of  $R_p(\text{th}) = 569 \text{ \AA}$  [11], are plotted as a function of  $T_i$ . As shown in Fig.1 at low temperatures the ratio of  $R_p(\text{ex})/R_p(\text{th})$  is approximately 1. For  $T_i$  close to 300°C, values determined for  $R_p$  are not reproducible because they depend strongly on the ion beam current density and dwell time. For  $T_i > 350^\circ\text{C}$ , the ratio  $R_p(\text{ex})/R_p(\text{th})$  is quite reproducible and is reduced to 85%. The corresponding

channeling spectra for the Si substrate (not shown) suggest that the observed decrease in  $R_p(ex)$  for  $T_i > 350^\circ C$  is related to the dynamic annealing process which occurs during implantation and is strongly dependent on  $T_i$ . Consequently the observed mobility of Er atoms for  $T_i > 300^\circ C$  might be interpreted as resulting from a defect mediated diffusion mechanism. This temperature is at least  $400^\circ C$  below the minimum temperature required for the thermally activated Er diffusion to become observable [10].

In order to get more insight into the ion beam induced diffusion effects the samples implanted with 145 keV Er<sup>+</sup> ions at  $RT < T_i < 200^\circ C$  were exposed to the thermal annealing as well as to the IBAA at the temperature of approximately  $300^\circ C$ . For the Er doses used in this work thermal annealing at  $300^\circ C$  does not modify the implanted Er distributions. At the same temperature of  $300^\circ C$  the IBAA does not lead to any measurable modification of the Er distribution for the Er dose of  $1 \times 10^{16}/\text{cm}^2$ . However, a significant Er redistribution occurs during IBAA for an Er dose of  $8 \times 10^{16}/\text{cm}^2$ . The IBAA was carried out in two steps, each step corresponding to a dose of  $5 \times 10^{15}$  As ions/ $\text{cm}^2$ . The resulting solid phase recrystallization and the Er segregation towards the surface are shown in Fig.2. The observed average growth rate corresponding to the first IBAA step is about 45 nm per  $5 \times 10^{15}$  ions/ $\text{cm}^2$ , a value which is about a factor 6 higher than that reported for (111) Si recrystallized using 600 keV Kr<sup>++</sup> at  $350^\circ C$  [12]. The growth rate slows considerably during the second IBAA step and no regrowth is observed during further

irradiation. This suggests that interface breakdown has occurred due to Er concentration reaching a limiting value [13]. The results shown on Fig.2 indicate that the redistribution of Er atoms occurring during the IBAA affects the totality of the Er profile in a manner which is not related to sputtering. The redistribution is also not related to the position of the recrystallization front. The mechanism of the observed concentration dependent, ion beam induced segregation of unbound Er atoms is not understood at the moment. It is believed however that both radiation induced phenomena described above may be responsible for the observed decrease in  $R_p(ex)$  at temperatures of  $300^\circ C$  or higher.

## 2. Formation of the polycrystalline phase.

Contact reactions between Si substrate and deposited Er metal have been shown to occur in a narrow temperature range around  $390^\circ C$  for (100) Si and  $480^\circ C$  for (111) Si [6], leading to the formation of a polycrystalline di-silicide as a first and apparently last phase [14]. Fig.3 shows the X-ray diffraction patterns for the (111) Si substrate implanted with the  $Er^+$  ions at the temperatures  $RT < T_i < 350^\circ C$ . The two principal lines corresponding to the diffraction angles of  $\theta_1 = 13.6^\circ$  and  $\theta_2 = 17.5^\circ$  have been identified as corresponding to the  $ErSi_2$  phase [15]. Both lines become observable for  $T_i > 250^\circ C$ . With the increasing  $T_i$  the relative intensity of the two lines vary as the  $\theta_2$  line becomes predominant, indicating that the growth is

orientation dependent.

Assuming that formation of the di-silicide phase leads to an increase of the surface binding energy and to a decrease of the sputtering coefficient [9] one would expect the retention  $R$  of Er to be strongly dependent on  $T_i$ . This effect is clearly seen on the Fig.4. The Er distributions in the "as implanted" state were measured in the center (a) and at the edge (b) of the same (111) Si sample pre-heated up to  $325^\circ\text{C}$  and implanted ( $1 \times 10^{17} / \text{cm}^2$ , 145 keV Er+) using beam current density of  $46 \mu\text{A}/\text{cm}^2$ . From the comparaison between the corresponding X-ray diffraction patterns (Fig.5) and those shown on the Fig.3 one may estimate the difference of temperature between a and b resulting from the beam heating to be close to  $50^\circ\text{C}$ . The corresponding difference in the  $R$  values is about 30%. The best-fitting values for the sputtering coefficient (calculated using the Profile code [11]) are  $Y(a)=3.82$  and  $Y(b)=5.2$ . We note that the theoretical value of  $Y$  corresponding to this experiment is  $Y=5.6$  [11].

### 3. Formation of the single crystal di-silicide phase.

The single crystal  $\text{ErSi}_2$  phase can be formed by implantation at  $T_i > 400^\circ\text{C}$ , followed by thermal annealing. The RBS/channeling spectra as well as the XTEM micrographs corresponding to the sample implanted at  $T_i = 500^\circ\text{C}$  with  $6 \times 10^{16} / \text{cm}^2$  of 170 keV Er+ and subsequently annealed at  $800^\circ\text{C}$  in vacuum are shown on Figs.6-7. It may be seen from the Fig.7a that the implantation process leads to formation of

precipitates of various sizes, correlated to the implanted Er distribution. From a preliminary analysis of TEM diffraction patterns (not shown) the precipitates are found to be small coherent precipitates of single crystalline  $\text{ErSi}_2$  phase. The corresponding RBS/channeling data show that in the "as implanted" state only a small fraction of precipitates are oriented along the [111] Si surface normal.

During thermal annealing at  $800^\circ\text{C}$  the Er distribution narrows due to Ostwald ripening [16] and separated islands of the buried single-crystalline  $\text{ErSi}_2$ , approximately  $250 \text{ \AA}^\circ$  thick, are formed (Fig.7b). The crystalline  $\text{ErSi}_2$  is now preferentially oriented with its [0001] direction parallel to the [111] surface normal. However, large undissolved  $\text{ErSi}$  precipitates remain on both sides of the buried layer. A temperature of  $800^\circ\text{C}$  appears to be the optimum annealing temperature because higher temperatures lead to an increase in the dechanneling yield and broadening of the Er distribution.

#### CONCLUSIONS

1. Implantation of  $\text{Er}^+$  ions into single crystal (111) Si at  $T_i > 280^\circ\text{C}$  results in formation of the polycrystalline  $\text{ErSi}_2$  phase. For  $T_i > 400^\circ\text{C}$  the  $\text{ErSi}_2$  crystallizes as coherent precipitates within a crystalline Si matrix.
2. Formation of the di-silicide phase results in an increase in the surface binding energy, causing a 30% decrease of the sputtering coefficient and a similar increase in the

retention of Er.

3. During thermal annealing the morphology of the implanted system dramatically changes and a discontinuous buried layer of the single crystalline ErSi is formed.

4. At implantation temperatures  $T_i > 300^\circ\text{C}$ , ion beam induced, defect mediated diffusion of the Er atoms strongly influences implanted Er distribution, causing a significant decrease in measured  $R_p$  values.

5. During ion beam assisted annealing at  $300^\circ\text{C}$ , a concentration dependent surface segregation of the unbound Er atoms is observed.

## DISCLAIMER

This report was prepared as an account of work sponsored by an agency of the United States Government. Neither the United States Government nor any agency thereof, nor any of their employees, makes any warranty, express or implied, or assumes any legal liability or responsibility for the accuracy, completeness, or usefulness of any information, apparatus, product, or process disclosed, or represents that its use would not infringe privately owned rights. Reference herein to any specific commercial product, process, or service by trade name, trademark, manufacturer, or otherwise does not necessarily constitute or imply its endorsement, recommendation, or favoring by the United States Government or any agency thereof. The views and opinions of authors expressed herein do not necessarily state or reflect those of the United States Government or any agency thereof.

REFERENCES:

- [1] F.Arnaud d'Avitaya, A.Perio, J.C.Oberlin, Y.Campidelli and J.A.Chroboczek  
Appl.Phys.Lett. 54, 2198 (1989)
- [2] F.Arnaud d'Avitaya, P.A.Badoz, Y.Campidelli, J.A.Chroboczek, J.Y.Duboz and A.Perio  
Thin Solid Films 184, 283 (1990)
- [3] K.N.Tu, R.D.Thompson, and B.Y.Tsaur  
Appl.Phys.Lett. 38, 626 (1981)
- [4] H.Norde, J.de Sousa Pires, D'Heurle, F.Pesavento, S.Peterson and P.A.Tove  
Appl.Phys.Lett. 38, 865 (1981)
- [5] J.A.Knapp and S.T.Picraux  
Appl.Phys.Lett. 48, 466 (1986)
- [6] J.E.Baglin, F.M.d'Heurle and C.S.Peterson  
Appl.Phys.Lett. 36, 594 (1980)
- [7] A.Golanski  
Appl.Surf.Sci. 43, 200 (1989)
- [8] T.L.Alford and J.C.Barbour  
Mat.Res.Symp.Proc. 1989, to be published
- [9] A.H.Van Ommen, J.J.M.Ottenheim, A.M.L.Theunissen and A.G.Mouwen  
Appl.Phys.Lett. 53, 669 (1988)
- [10] J.E.E.Baglin, F.M.d'Heurle and C.S.Peterson  
J.Appl.Phys. 52, 2841 (1981)
- [11] A.J.Armini, S.N.Bunker  
Mat.Sci.Eng. A115, 67 (1989)
- [12] F.Priolo, C.Spinella, A.La Ferla, E.Rimini and G.Ferla  
Appl.Surf.Sci. 43, 178 (1989)
- [13] S.J.Pennycook  
Mat.Res.Symp.Proc.Vol.147, 45 (1989)
- [14] R.D.Thompson, B.Y.Tsaur and K.N.Tu  
Appl.Phys.Lett. 38, 535 (1981)
- [15] Standard Powder Diffraction Pattern no.12-37
- [16] In Physical Chemistry, An Advanced Treatise, Vol.X  
W.Jost, Editor  
Academic Press, New York, London, 748 (1970)

FIGURE CAPTIONS:

FIG.1: Normalized ratio  $R_p(ex)/R_p(th)$  for 145 keV Er in Si plotted as a function of the implantation temperature ( $T_i$ ).

FIG.2: RBS/channeling spectra for the  $\langle 111 \rangle$  Si implanted with 145 keV Er+ at  $RT < T_i < 200^\circ C$  and subsequently exposed to IBAA at  $300^\circ C$  using the doses of  $5 \times 10^{15}/cm^2$  and  $1 \times 10^{16}/cm^2$  of 1.02 MeV As ions. The "beam off" spectra correspond to the thermal annealing at  $300^\circ C$ .

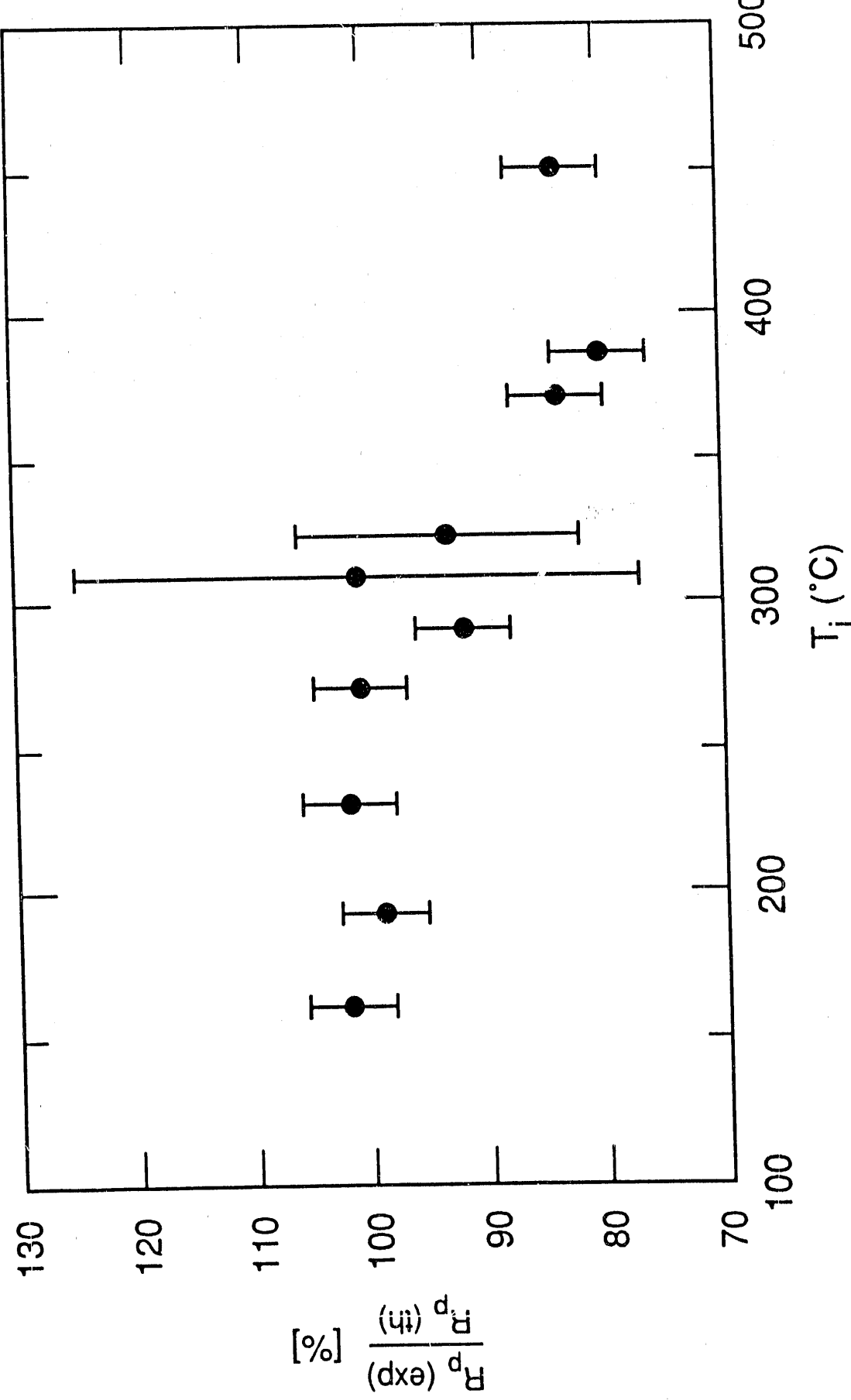
FIG.3: X-ray diffraction patterns for Er implanted  $\langle 111 \rangle$  Si for  $RT < T_i < 350^\circ C$ .

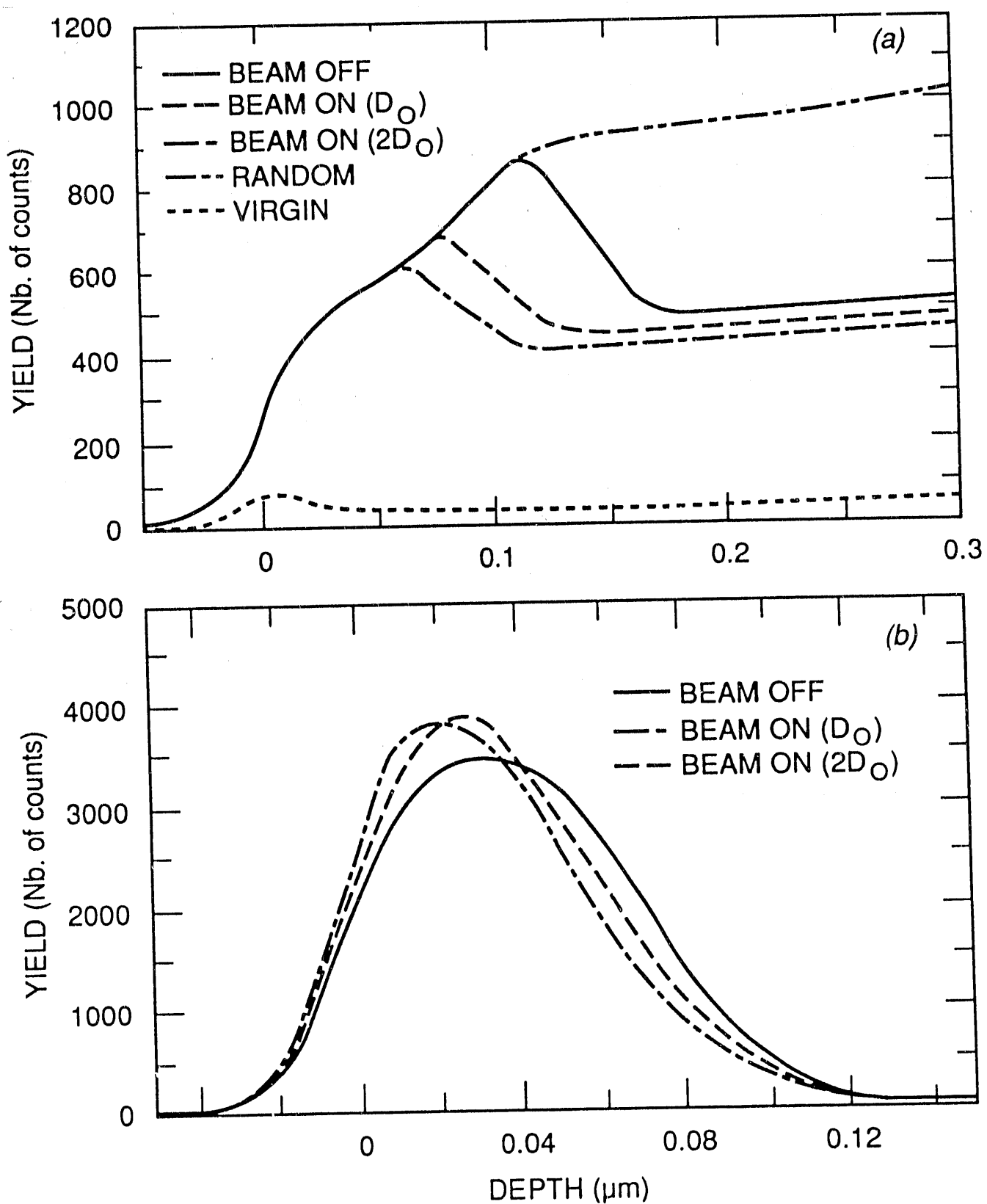
FIG.4: The effect of  $ErSi_2$  phase formation during implantation of Er (145 keV,  $1 \times 10^{16}/cm^2$ ) on the retention R of the implanted Er. The sample pre-heated up to  $T_i = 325^\circ C$  was exposed to the beam heating. The resulting difference between the surface temperatures in the sample center (a) and edge (b) may be close to  $50^\circ C$ . The corresponding R values are 86% and 54%. The RBS spectrum for  $1 \times 10^{16}/cm^2$  ( $R=100\%$ ) is shown for comparison.

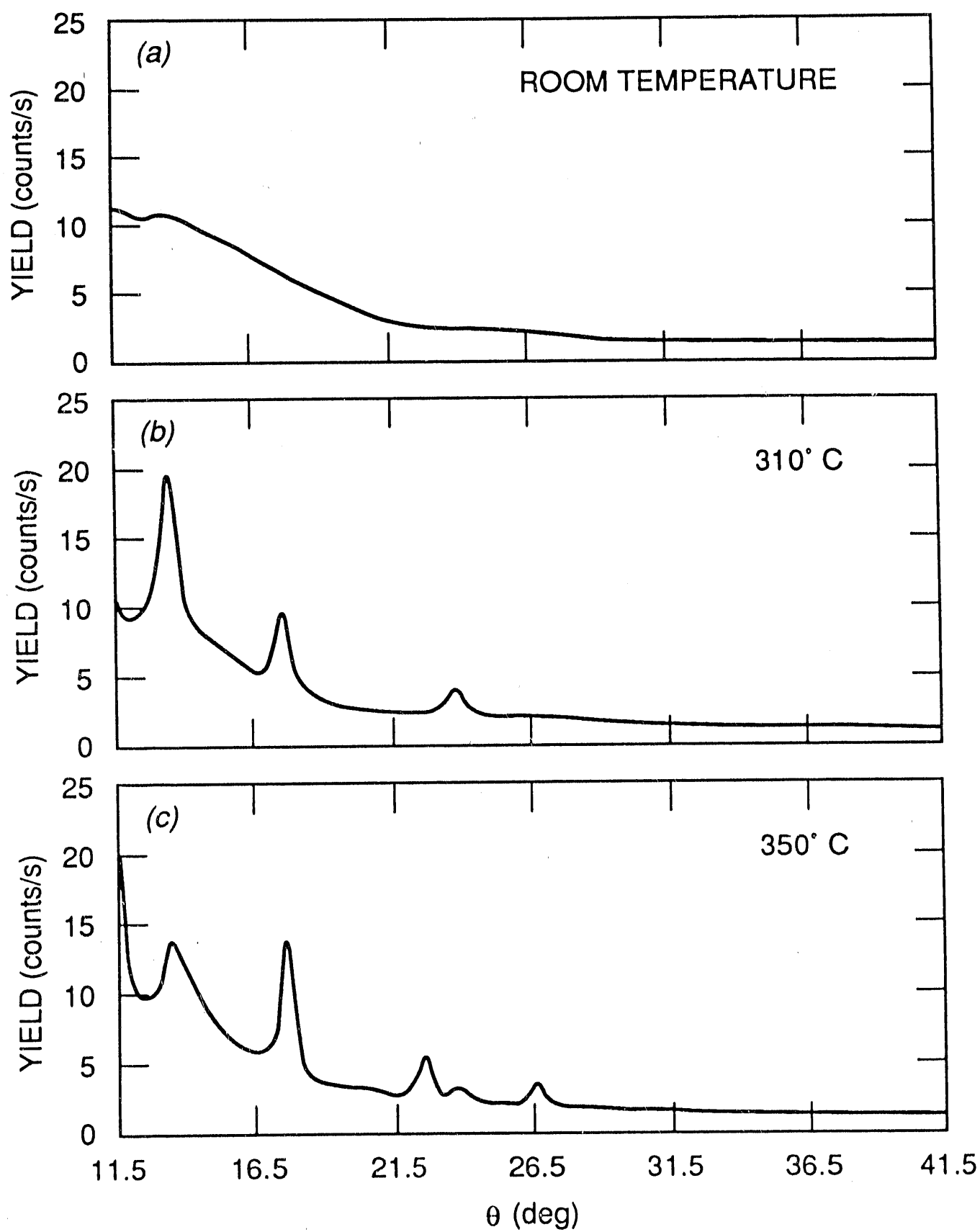
FIG.5: X-ray diffraction patterns corresponding to the RBS spectra shown on the Fig.4.

FIG.6: RBS/channeling spectra for Er (a) and Si substrate (b), corresponding to the "as implanted" and annealed  $\langle 111 \rangle$  Si samples, implanted by Er (170 keV,  $6 \times 10^{16}/cm^2$ ) at  $T_i = 500^\circ C$ .

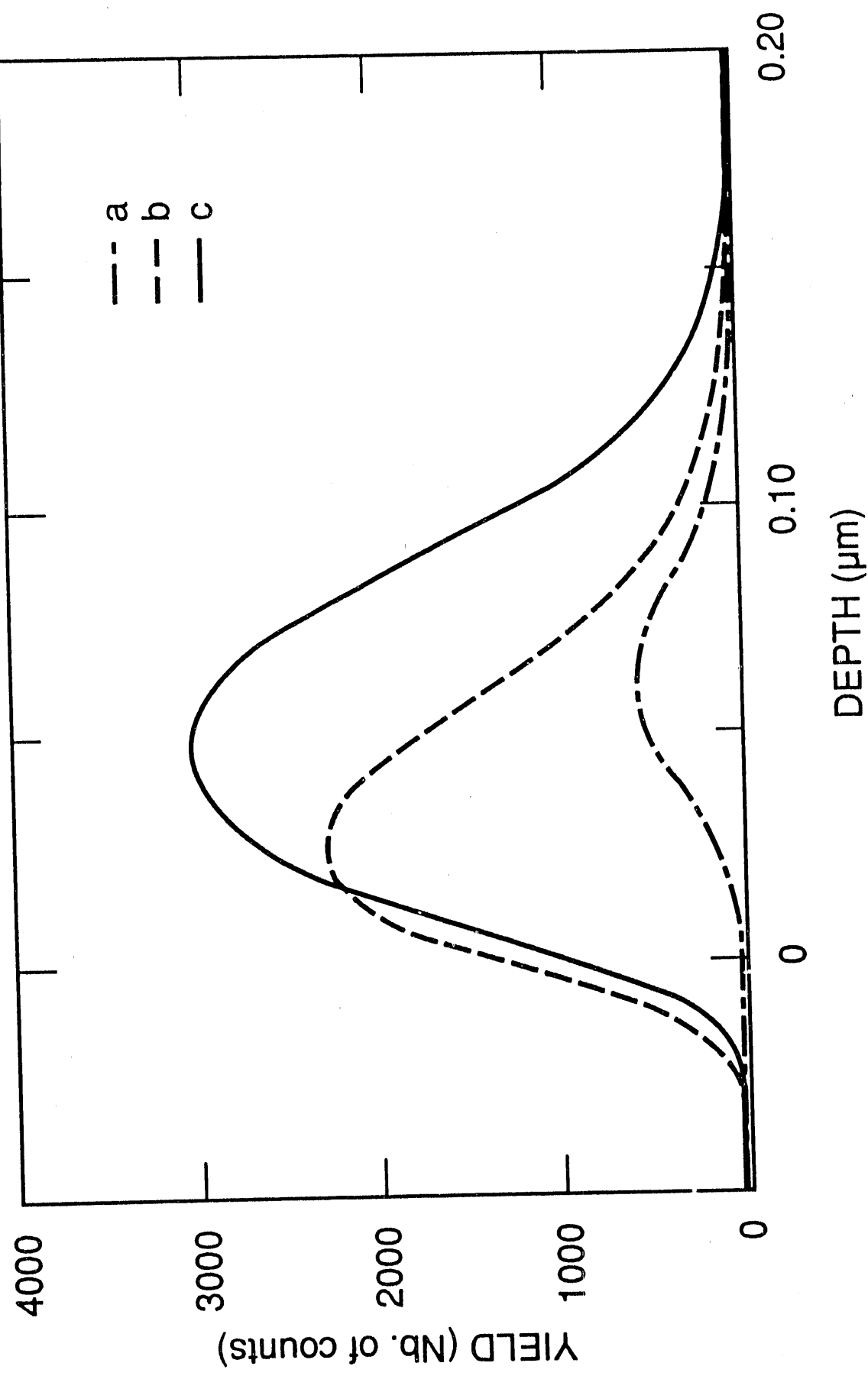
FIG.7: XTEM micrographs corresponding to the RBS spectra shown on the Fig.6: (a) coherent  $\text{ErSi}_2$  precipitates in the as implanted state; (b) morphology of the system after annealing at  $800^\circ\text{C}$  in vacuum.



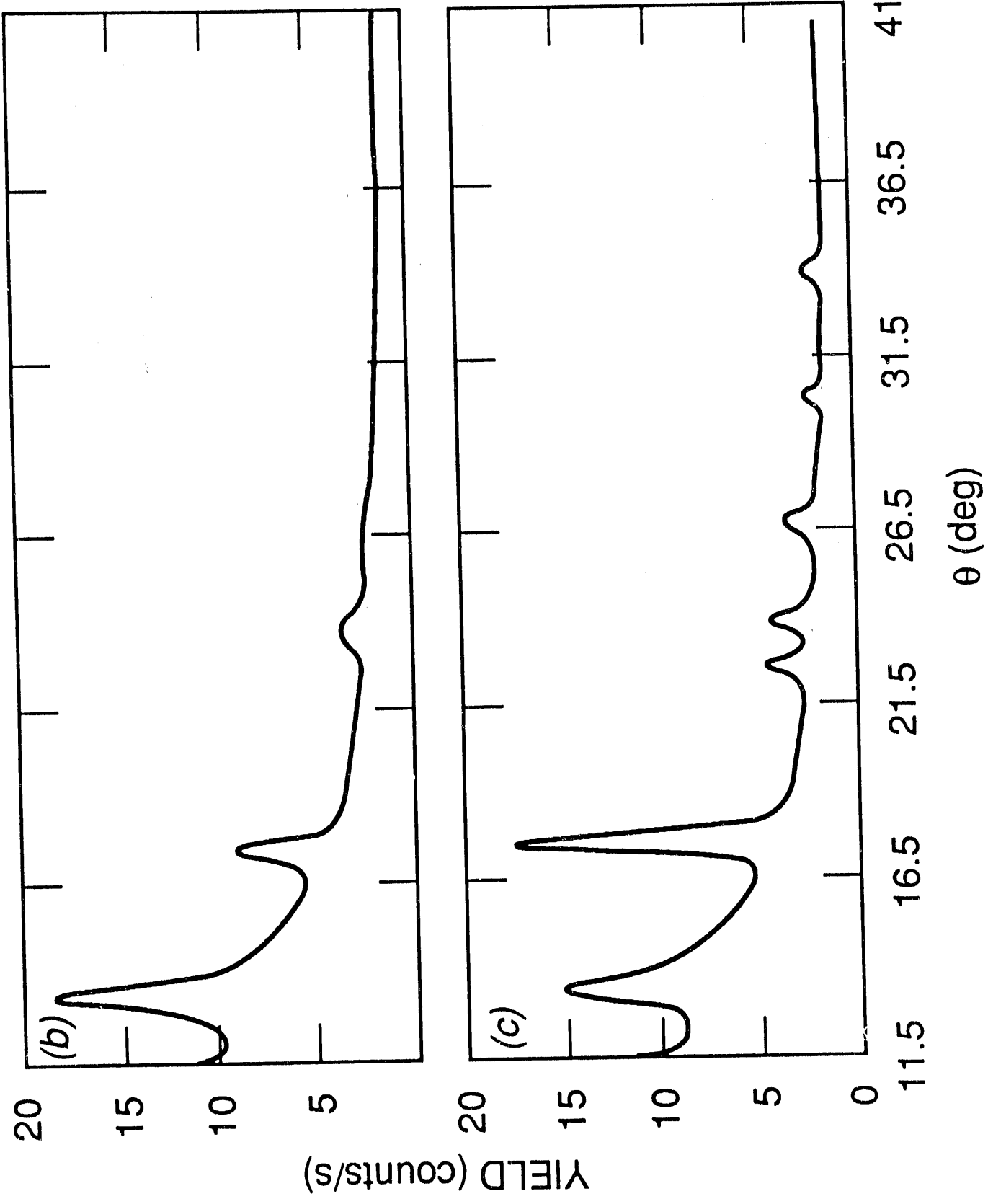


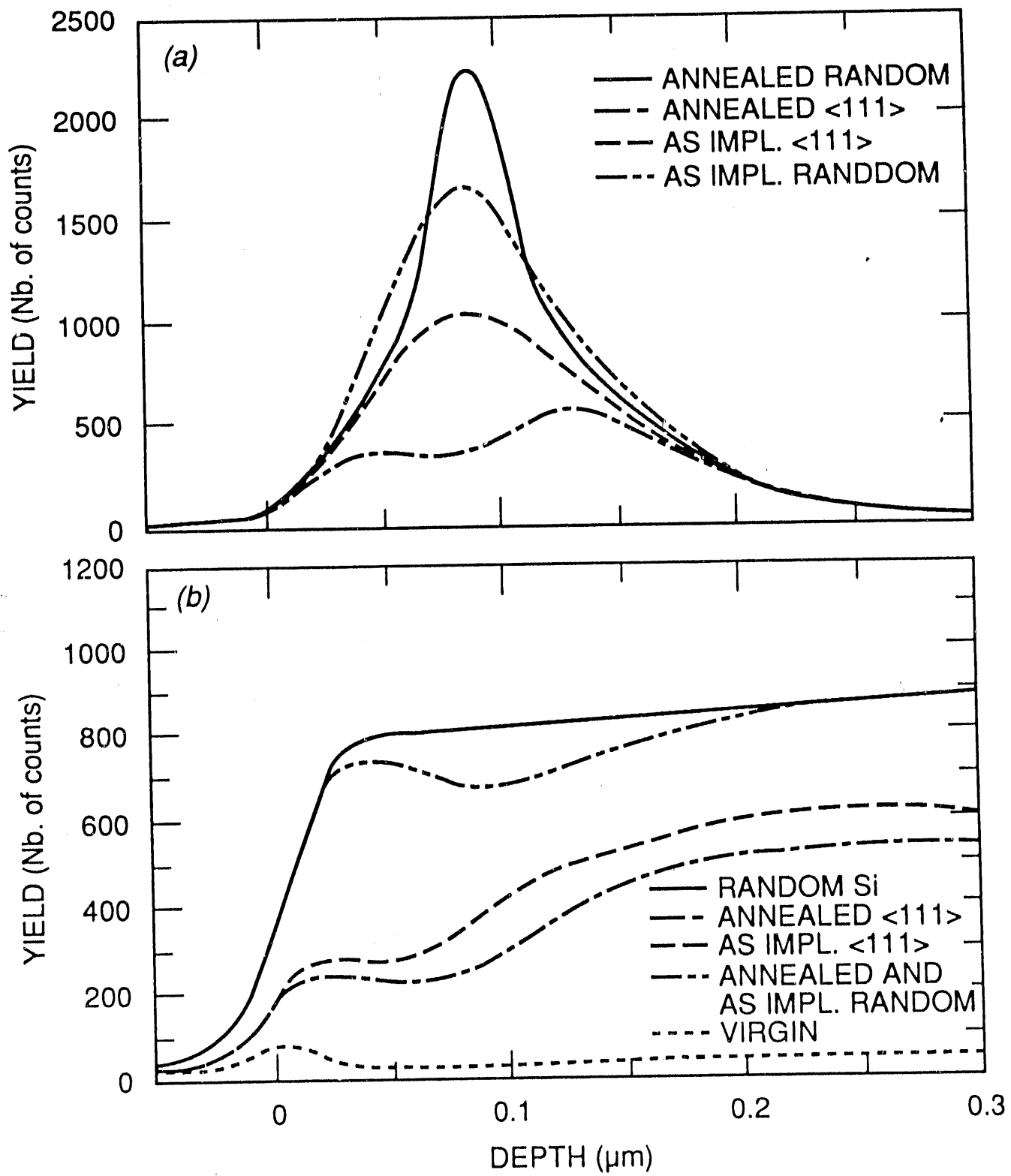


ORNL-DWG 90M-14389



ORNL-DWG 90M-14388





**END**

**DATE FILMED**

**12/13/90**

